

Journal of Systematic Palaeontology

Publication details, including instructions for authors and subscription information:

<http://www.tandfonline.com/loi/tjsp20>

New pelomedusoid turtles from the late Palaeocene Cerrejón Formation of Colombia and their implications for phylogeny and body size evolution

Edwin A. Cadena ^{a b c}, Daniel T. Ksepka ^{a d}, Carlos A. Jaramillo ^c & Jonathan I. Bloch ^b

^a Department of Marine, Earth and Atmospheric Sciences, North Carolina State University, Raleigh, North Carolina, 27695-8208, USA

^b Florida Museum of Natural History, Dickinson Hall, University of Florida, Gainesville, Florida, 32611-7800, USA

^c Smithsonian Tropical Research Institute, Balboa, Ancon AA, 0843-03092, Panama

^d Department of Paleontology, North Carolina Museum of Natural Sciences, Raleigh, North Carolina, 26701, USA

Available online: 17 May 2012

To cite this article: Edwin A. Cadena, Daniel T. Ksepka, Carlos A. Jaramillo & Jonathan I. Bloch (2012): New pelomedusoid turtles from the late Palaeocene Cerrejón Formation of Colombia and their implications for phylogeny and body size evolution, *Journal of Systematic Palaeontology*, 10:2, 313-331

To link to this article: <http://dx.doi.org/10.1080/14772019.2011.569031>

PLEASE SCROLL DOWN FOR ARTICLE

Full terms and conditions of use: <http://www.tandfonline.com/page/terms-and-conditions>

This article may be used for research, teaching, and private study purposes. Any substantial or systematic reproduction, redistribution, reselling, loan, sub-licensing, systematic supply, or distribution in any form to anyone is expressly forbidden.

The publisher does not give any warranty express or implied or make any representation that the contents will be complete or accurate or up to date. The accuracy of any instructions, formulae, and drug doses should be independently verified with primary sources. The publisher shall not be liable for any loss, actions, claims, proceedings, demand, or costs or damages whatsoever or howsoever caused arising directly or indirectly in connection with or arising out of the use of this material.

New pelomedusoid turtles from the late Palaeocene Cerrejón Formation of Colombia and their implications for phylogeny and body size evolution

Edwin A. Cadena^{a,b,c,*}, Daniel T. Ksepka^{a,d}, Carlos A. Jaramillo^c and Jonathan I. Bloch^b

^aDepartment of Marine, Earth and Atmospheric Sciences, North Carolina State University, Raleigh, North Carolina 27695-8208, USA;

^bFlorida Museum of Natural History, Dickinson Hall, University of Florida, Gainesville, Florida 32611-7800, USA; ^cSmithsonian Tropical Research Institute, Balboa, Ancon AA 0843-03092, Panama; ^dDepartment of Paleontology, North Carolina Museum of Natural Sciences, Raleigh, North Carolina 26701, USA

(Received 30 August 2010; accepted 5 November 2010; printed 16 May 2012)

Pelomedusoides comprises five moderate-sized extant genera with an entirely Southern Hemisphere distribution, but the fossil record of these turtles reveals a great diversity of extinct taxa, documents several instances of gigantism, and indicates a complex palaeobiogeographical history for the clade. Here, we report new pelomedusoid turtle fossils from the late Palaeocene Cerrejón Formation of Colombia. The most complete of these is represented by a large skull (condylobasal length = 16 cm) and is described as *Carbonemys cofrinii* gen. et sp. nov. (Podocnemidae). *Carbonemys* is incorporated into a parsimony analysis utilizing a modified morphological character matrix designed to test relationships within Panpelomedusoides, with the addition of molecular data from seven genes (12S RNA, cytochrome b, ND4, NT3, R35, RAG-1 and RAG-2) drawn from previous studies of extant Podocnemidae. *C. cofrinii* is recovered within Podocnemidae in the results of both morphology-only and combined morphological and molecular (total evidence) analyses. However, molecular data strongly impact the inferred relationships of *C. cofrinii* and several other fossil taxa by altering the relative positions of the extant taxa *Peltecephalus* and *Erymnochelys*. This resulted in *C. cofrinii* being recovered within the crown clade Podocnemidae in the morphology-only analysis, but outside of Podocnemidae in the combined analysis. Two Panpodocnemid turtle taxa of uncertain affinities are represented by new diagnostic shell material from the Cerrejón Formation, though we refrain from naming them pending discovery of associated cranial material. One of these shells potentially belongs to *C. cofrinii* and represents the second largest pleurodiran turtle yet discovered. Analysis of pelomedusoid body size evolution suggests that climatic variation is not the primary driver of major body size changes. Cerrejón turtles also demonstrate that at least two major subclades of Podocnemidae were already in place in the neotropics by the Early Cenozoic.

Keywords: Pleurodira; Pelomedusoidea; Testudines; gigantism; total evidence

Introduction

The late Palaeocene (58–55 Ma) Cerrejón Formation of northernmost Colombia (Fig. 1A) has yielded some of the most interesting discoveries of neotropical fossil reptiles in the last decade, including the largest known snake *Titanoboa cerrejonensis* (Head *et al.* 2009), the diminutive short-snouted dyrosaurid *Cerrejonisuchus improcerus* (Hastings *et al.* 2010), and the podocnemid turtle *Cerrejonemys wayuunaiki* (Cadena *et al.* 2010). These fossils have provided important information for palaeoclimatic reconstructions, phylogenetic analyses and palaeobiogeographical hypotheses (see references cited above). Here we report new turtles from the Cerrejón Formation, including a new genus and species of Podocnemidae represented by a large skull, and two distinct shell morphotypes belonging to panpodocnemids of uncertain affinities.

The fossils described here were recovered from a layer of claystone underlying Coal Seam 90 in the middle part of the brackish-continental Cerrejón Formation (Bayona *et al.* 2004) (Fig. 1B). The well-preserved palynoflora of the Cerrejón Formation includes *Foveotricolpites perforatus* and *Bombacacidites annae*, part of a palynological assemblage indicating a middle–late Palaeocene age (palynological zone Cu-02; Jaramillo *et al.* 2007).

Institutional abbreviations

UF/IGM: Vertebrate Paleontology Florida Museum of Natural History, University of Florida, Gainesville, USA / Instituto Colombiano de Investigaciones Mineras INGEOMINAS, Bogotá, Colombia; **MCZ:** Museum of Comparative Zoology, Harvard University, Boston, USA.

*Corresponding author. Email: eacadena@ncsu.edu

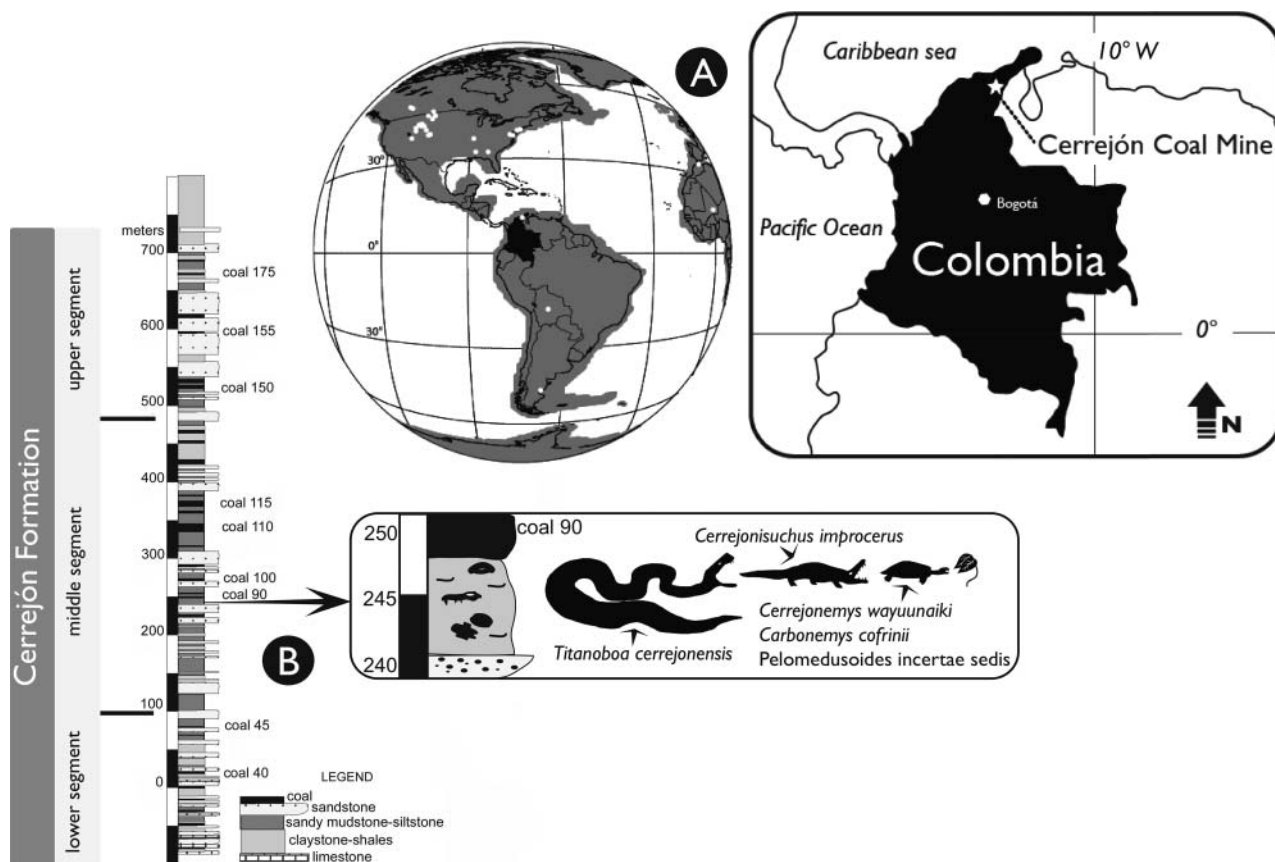


Figure 1. A, map of Colombia showing the Cerrejón Coal Mine locality, with stratigraphic column for the upper Palaeocene Cerrejón Formation. Globe depicts land mass reconstructions for the Palaeocene (in grey) with white dots representing fossil occurrences of Testudines. Distributional data were downloaded from the Paleobiology Database on 20 May 2010, using the group name 'Testudines' and the following parameters: time intervals = 55 Ma, region = western hemisphere. B, stratigraphical column of the Cerrejón Formation, modified from Bayona *et al.* (2004). The 10-metre section of the middle segment of Cerrejón Formation, showing the claystone layer yielding *Carbonemys cofrinii* and the other two turtle taxa described here is enlarged.

Systematic palaeontology

Testudines Batsch, 1788

Panpleurodira Joyce *et al.*, 2004

Pleurodira Cope, 1864 *sensu* Joyce *et al.*, 2004

Panpodocnemididae Joyce *et al.*, 2004

Podocnemidae Joyce *et al.*, 2004

Genus ***Carbonemys*** gen. nov.

Type species. *Carbonemys cofrinii* sp. nov.

Diagnosis. As for type species (below).

Derivation of name. Combining 'Carbon' (Latin, *Carbo*, coal) with 'emys' (Greek, freshwater turtle).

Carbonemys cofrinii sp. nov.
(Figs 2, 3)

Holotype. UF/IGM 41, nearly complete skull (Figs 2, 3).

Diagnosis. *Carbonemys cofrinii* differs from all other podocnemids by the presence of the following apomorphies: (1) a prefrontal–postorbital contact that excludes the frontals from the orbital margin; (2) a reduced basisphenoid with very short medial incursion between the pterygoids; and (3) a posteriorly wide snout which becomes abruptly narrow anteriorly, particularly at the premaxillary region.

Derivation of name. In honour of Dr David Cofrin, one of the most important contributors to our palaeontological expeditions and curatorial activities.

Occurrence. La Puente Pit, Cerrejón Coal Mine, Guajira Peninsula, Colombia, (11° 08' 30" N, 72° 33' 20" W). Single claystone layer, middle part of the Cerrejón Formation; late Palaeocene (58–55 Ma), palynological zone Cu-02 (Jaramillo *et al.* 2007).

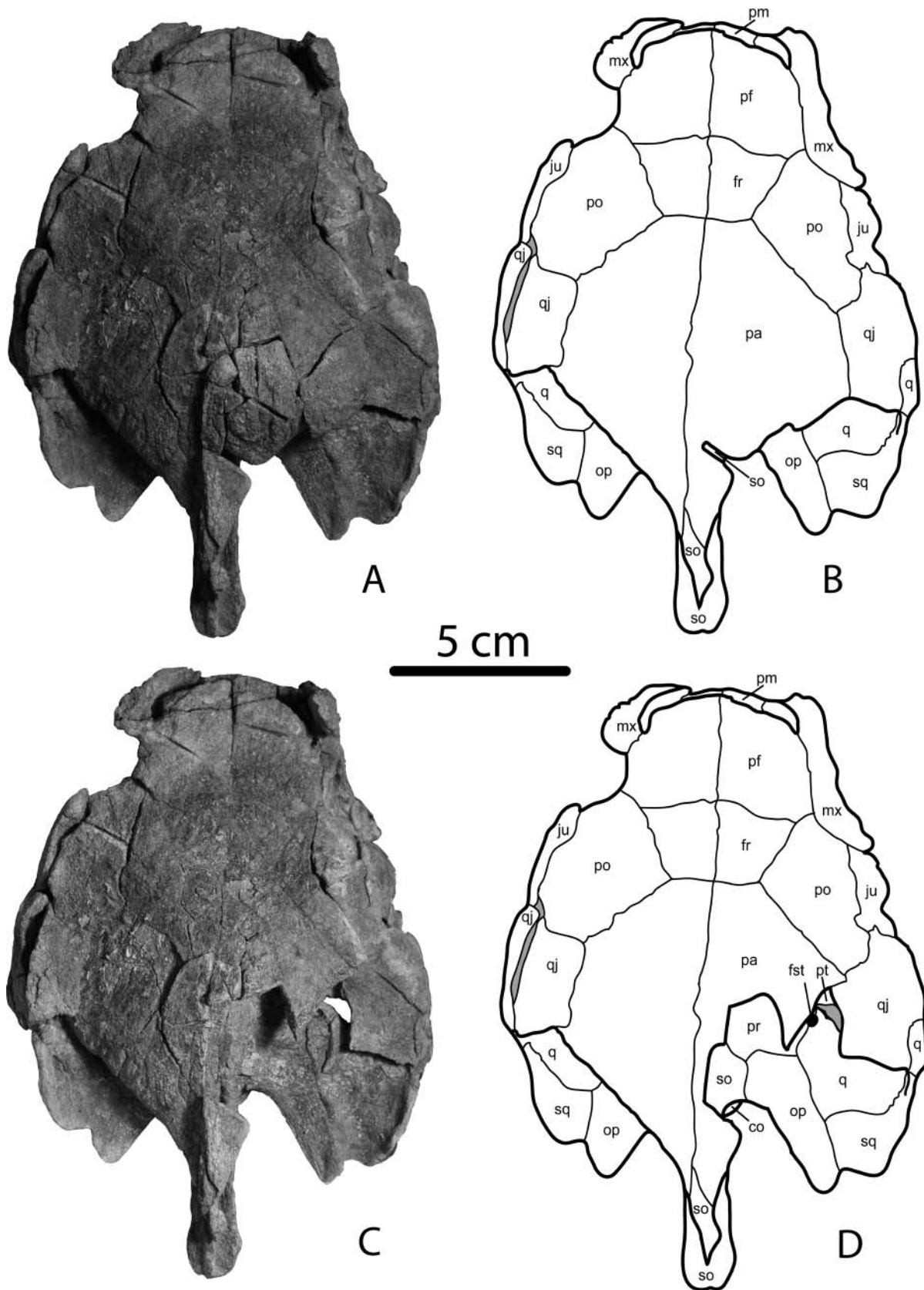


Figure 2. *Carbonemys cofrinii* sp. nov., UF/IGM 41, holotype. **A, B**, complete skull in dorsal view; **C, D**, skull without a portion of the parietal, showing the bones at the roof of the otic chamber. Abbreviations: fr, frontal; fst, foramen stapedio temporale; ju, jugal; mx, maxilla; op, opisthotic; pa, parietal; pf, prefrontal; po, postorbital; pr, prootic; q, quadrate; qj, quadratojugal; so, supraoccipital; sq, squamosal.

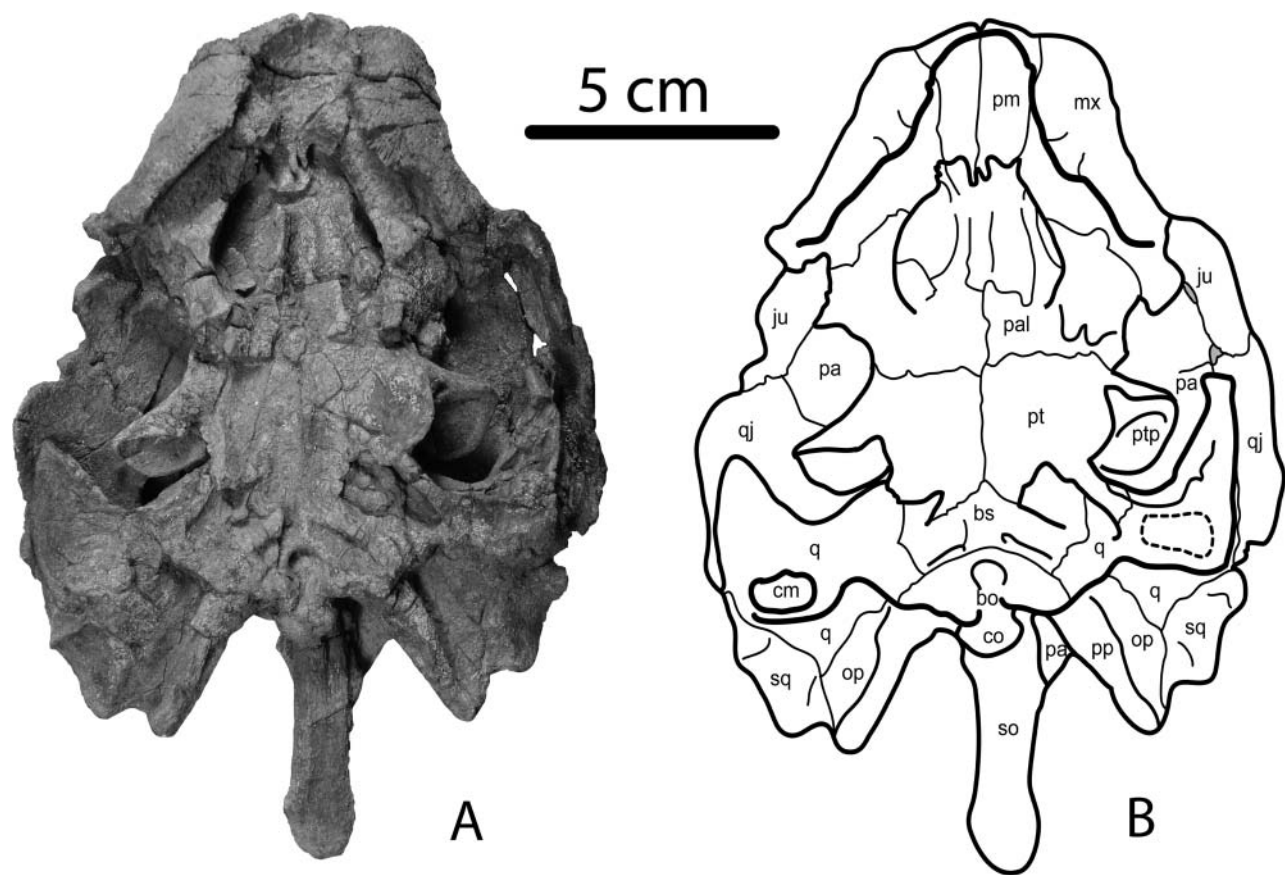


Figure 3. *Carbonemys cofrinii* sp. nov., UF/IGM 41, holotype. **A, B**, complete skull in ventral view. Abbreviations: bo, basioccipital; bs, basisphenoid; cm, condylus mandibularis; co, condylus occipitalis; ju, jugal; mx, maxilla; op, opisthotic; pa, parietal; pal, palatine; pm, premaxilla; pp, processus paroccipitalis; pr, prootic; pt, pterygoid; ptp, processus trochlearis pterygoidei; q, quadrate; qj, quadratojugal; so, supraoccipital; sq, squamosal.

Comparative description. The type and only skull of *Carbonemys cofrinii* is almost complete (see Table 1 for measurements) but is considerably crushed dorsally. The snout is both wide and relatively long. The maxillae are

much larger than those in any other podocnemid species, except for *Caninemys tridentada* which has the largest and thickest maxillae of any member of the clade (Meylan *et al.* 2009). In dorsal view the temporal emargination (better

Table 1. Measurements in centimetres for: UF/IGM 41, holotype of *Carbonemys cofrinii*; UF/IGM 71, Pelomedusoides shell taxon A; UF/IGM 72, UF/IGM 73, UF/IGM 74, UF/IGM 75, Pelomedusoides shell taxon B. Abbreviations: MLI: maximum length indicated as I in Gaffney *et al.* (2006, fig. 315); MWI: maximum width indicated as B in Gaffney *et al.* (2006, fig. 315); ML: maximum length; LE: length estimated for complete carapace; MW: maximum width; WE: width estimated for complete plastron; T: average thickness.

		MLI	MWI	ML	LE	MW	WE	T
UF/IGM 41	Skull	21	13	—	—	—	—	—
UF/IGM 71	Carapace	—	—	173	180	157	160	1.2
	Plastron	—	—	52	100	132	120	1.4
UF/IGM 72	Carapace	—	—	19.2	17.3	21	18	0.5
	Plastron	—	—	18.1	11.2	18.1	13	0.5
UF/IGM 73	Carapace	—	—	10.3	19	7.5	13	0.4
	Plastron	—	—	7.2	15	5.9	11	0.4
UF/IGM 74	Carapace	—	—	8.1	13	9.0	10	0.3
	Plastron	—	—	6.4	9.5	7.8	7.8	0.3
UF/IGM 75	Nuchal bone	—	—	2.4	2.4	2.2	2.2	0.3

preserved on the left side) extends very far posteriorly, with straight tapering margins completely covering the roof of the otic chamber. The emargination is comparatively more advanced than in *Podocnemis* spp., *Cerrejonemys wayuunaiki*, *Bauruemys elegans* and aff. *Roxochelys vilavilensis* but slightly less advanced than in *Erymnochelys madagascariensis*, *Peltocephalus dumerilianus*, *Shweboemys antiqua*, *Neochelys arenarum*, *Bairdemys venezuelensis*, *B. harsteini*, *B. winklerae*, *Dacquemys paleomorpha* and some specimens of *P. erythrocephala* (Gaffney *et al.* 2006). The extent of cheek emargination is not clearly visible in the holotype of *C. cofrinii* due to crushing. However, it is clear that the degree of emargination is much less than in *Peltocephalus dumerilianus* and *E. madagascariensis*, and that a contact between the jugal and the quadrate is lacking.

Nasal bones are absent as in all other pelomedusoids (Joyce 2007). The prefrontals are large, flat elements (lacking a groove), and are slightly wider than long. The anterior protrusion of the prefrontals completely covers the apertura narium externa, ending in a slightly convex tip as in *Dacquemys paleomorpha*, *Stereogenys cromeri*, *Bairdemys* spp., *Shweboemys antiqua* and especially *Peltocephalus dumerilianus* and *Erymnochelys madagascariensis* (Gaffney *et al.* 2006). Posterolaterally, the prefrontals contact the postorbitals, a character that is apomorphic for *C. cofrinii* among pelomedusoids. In other pelomedusoids the prefrontals contact the frontals posteriorly but do not contact the postorbitals. The prefrontals are reduced to small elements in *Bauruemys elegans*, aff. *Roxochelys vilavilensis* and *Podocnemis* spp. In contrast to other podocnemids, the frontals of *C. cofrinii* are small and excluded from the orbital margin by the prefrontal–postorbital contact. The orbits of *C. cofrinii* are crushed, but appear to be more laterally oriented as in *D. paleomorpha*, *S. cromeri*, *Bairdemys* spp., *S. antiqua*, *P. dumerilianus* and *E. madagascariensis*, rather than dorsally oriented as in *Podocnemis* spp., *B. elegans*, aff. *R. vilavilensis*, and *Caninemys tridentata* (Meylan *et al.* 2009). The postorbitals are large and contact the quadratojugals posteriorly, as in all other podocnemids except for *Podocnemis* spp. and *C. wayuunaiki* (Cadena *et al.* 2010). The parietals are the largest roofing elements of the skull. They contact the postorbitals, frontals and quadratojugals as in other podocnemids. However, the parietal–jugal contact seen in *Podocnemis* spp. and *C. wayuunaiki* is absent. The supraoccipital is restricted to a position between the parietals in dorsal view as in other podocnemids.

Breakage of the right parietal exposes the contact between the supraoccipital, right prootic, opisthotic and squamosal. These elements share a pattern of contacts similar to other panpodocnemids. The foramen stapediotemporale is large and positioned between the prootic and the quadrate. The jugal and quadratojugal are crushed, but both show a pattern of contacts with the maxilla and the quadrate similar to that in other podocnemids.

In ventral view, the premaxillae have a highly concave, anteroposteriorly broad triturating surface. The vomer is not preserved, but a serrate articular surface at the posterior margin of the premaxillae indicates that it was present in life. There is no evidence for the foramen prepalatinum in *Carbonemys cofrinii*. This foramen is also absent in *Dacquemys paleomorpha*, *Stereogenys cromeri* and *Peltocephalus dumerilianus*, and variably present/absent in *Podocnemis expansa* (Cadena *et al.* 2010). As mentioned above, the maxillae are very large compared to most other podocnemids. Unlike *Caninemys tridentata*, the maxillae in *Carbonemys cofrinii* lack prominent tooth-like processes. The triturating surface in *C. cofrinii* is formed by the premaxillae, maxillae and palatines. The surface is broad and smooth, lacking primary or accessory ridges. The palatines contact the maxillae laterally and the pterygoids posteriorly. *C. cofrinii* lacks a foramen palatinum posterius between the palatines and the pterygoids as in *D. paleomorpha*, *Shweboemys antiqua*, *Stereogenys cromeri* and *Bairdemys sanchezi* (Cadena *et al.* 2010). Palatal architecture of *C. cofrinii* indicates a relatively narrow rostrum, similar to but slightly wider than that of *P. dumerilianus*.

The pterygoids contact the palatines anteriorly, the basisphenoid posteriorly, and the quadrates posterolaterally via a strong quadrate process as in *Caninemys tridentata* and other podocnemids (Meylan *et al.* 2009). The processus trochlearis pterygoidei is large and laterally directed into the centre of the fossa temporalis, as in other podocnemids except for *Bauruemys elegans*, aff. *Roxochelys vilavilensis* and *Peltocephalus dumerilianus*, all of which have a processus projected more obliquely with respect to the midline of the skull. At the posterior aspect of the pterygoids, the cavum pterygoidei is very well developed and deep. The pterygoid wings are broken, but the preserved portions indicate that they were elongate, potentially covering the cavum pterygoidei as in other podocnemids. Particularly extensive wings are present in *Podocnemis* spp., *Peltocephalus dumerilianus*, *Cerrejonemys wayuunaiki* and *E. madagascariensis*. The basisphenoid is small with a very short medial incursion between the pterygoids, contrasting with other panpodocnemids which have a larger element that broadly separates the pterygoids posteromedially. The basioccipital is slightly wider than the basisphenoid, and contacts the basisphenoid anteriorly, quadrates laterally, and the exoccipital dorsally. The basioccipital has an apomorphically deep circular notch at the middle of the element. A shallower notch occurs in other podocnemids.

The quadrates of *Carbonemys cofrinii* possess the same sutural contacts as in other podocnemids. The cavum tympani is crushed but preserves a very small antrum postoticum as in most other podocnemids, particularly *Podocnemis expansa*. The condylus mandibularis is well preserved on the left quadrate. The condyle is much wider than long, with straight to concave anterior and posterior edges as in other podocnemids, except in *Podocnemis* spp.

and probably *Cerrejonemys wayuunaiki* (see Cadena *et al.* (2010) for discussion about the condylus mandibularis). The opisthotic has a medially narrow and elongated processus paroccipitalis that projects beyond the squamosal as in other podocnemids, except for *Shweboemys antiqua* and *Bairdemys* spp. The supraoccipital includes a long crista supraoccipitalis that is uniform in width along its ventral base.

Pelomedusoides shell taxon A
(Fig. 4)

Comparative description. A single nearly complete, somewhat crushed, articulated carapace and plastron (UF/IGM 71; Fig. 4) was recovered from the same stratigraphical horizon as the holotype skull of *Carbonemys cofrinii*. This specimen can be referred to *Pelomedusoides* based on the absence of the cervical scale, and is notable for its very large size (173 cm maximum carapace length). In fact, the size of this specimen is not far off from what one might predict for the shell of *C. cofrinii*, but lack of direct association makes it impossible to attribute the shell confidently to that taxon pending further discoveries. The skull differs from all other known *Pelomedusoides* in: (1) the presence of a long and very narrow knob developed on the medial portion of costal 8 and projected slightly onto the peripherals; (2) striated sculpture on the dorsal surface of neural 8, costal 7 and suprapygals 1; and (3) posterior peripherals including the pygal having a medial knob parallel to the lateral margins.

Portions of the anterior left peripherals and costals and posterior right peripherals are either not preserved or crushed, and neurals two and three were not recovered. The carapace is oval in dorsal view with a shallow embayment at the nuchal area that contrasts sharply with the deep notch present in *Stupendemys geographicus* (MCZ4376) (Fig. 5). Anteriorly, the nuchal is pentagonal in shape, as wide as long, and completely flat. This shape is shared by other podocnemids, except *S. geographicus*, which possess a thickened and strongly upturned anterior margin of the nuchal (Wood 1976). The neural series is composed of eight elements. Neural 1 is rectangular and very wide, as in *S. geographicus*. Neurals 4–8 are hexagonal. *Pelomedusoides* shell taxon A and *S. geographicus* possess a second suprapygals element, resulting in complete separation of the posterior costal elements, as is also the condition in *Araripemys barretoii*, *Dortoka vasconica* and platychelyids. Suprapygals 2 is longer and narrower than suprapygals 1 in both *Pelomedusoides* shell taxon A and *S. geographicus*. As in other pelomedusoids, neural 1 contacts only costal 1 laterally, and neural 2 contacts costal 1 anterolaterally. Peripherals 1–4 are trapezoidal and increase in size posteriorly. They are smaller than the nuchal, as in other pelomedusoids except *S. geographicus*, which possess a peripheral 1 larger than the nuchal. Axillary buttresses are

present on the ventral surface of the carapace, extending from the posterolateral surface of costal 1 to peripheral 3 as in podocnemids, except *S. geographicus* which has axillary buttresses projected onto the peripheral 2. At the posterior region of the carapace a pronounced radial knob is present, almost parallel to the sutures between the peripherals. This knob is developed from the medial portion of costal 8 and is projected slightly onto the anterior area of peripherals. On the dorsal surface of neural 8, costal 7 and suprapygals 1 a striated pattern is also well preserved. All posterior peripherals including the pygal have a medial knob parallel to the lateral margins. In contrast, *S. geographicus* has a very irregular dorsal surface of the carapace but there is no evidence of knobs. As in all other pelomedusoids the cervical scale is absent. The pleural scales of *Pelomedusoides* shell taxon A cover a major portion of peripherals as in *S. geographicus*, as is also the condition in most bothremydids. Less marked extension of the pleurals over the peripherals is the typical condition in podocnemids.

Only the posterior portion of the plastron is preserved. The preserved margins of the plastron suggest that it was approximately 60% the length of the carapace, comparable to the proportions in other podocnemids. The preserved left mesoplastron is slightly longer than wide. The xiphiplastron has an open U-shaped anal notch. The femoroabdominal sulcus ends at the lateral notch of the hypoplastron. The femoroanal sulcus is also clearly visible over both xiphiplastron.

Pelomedusoides shell taxon B
(Fig. 6)

Material. UF/IGM 72, carapace and plastron (Fig. 6A–F). UF/IGM 73, partially articulated shell (Fig. 6G–J). UF/IGM 74, partially articulated shell (Fig. 6K–P). UF/IGM 75, nuchal and left costal 1 (Fig. 6Q–R).

Comparative description. Four small shells recovered from the same stratigraphical horizon as *Carbonemys cofrinii* appear to belong to a single taxon. Again, because no associated skulls were recovered, we refrain from diagnosing a new taxon. However, ‘*Pelomedusoides* shell taxon B’ can be assigned to *Pelomedusoides* based on the absence of a cervical scale. It differs from the other turtles from the Cerrejón Formation and other pelomedusoids by the combination of the following characteristics: (1) lack of neural series; (2) only seven pair of costals; and (3) humeral scales completely separated medially by the intergular.

UF/IGM 72 (Fig. 6A–F) is an articulated small shell (see Table 1 for measurements), with most of the posterior margin missing. The nuchal bone is pentagonal in shape, slightly longer than wide, with the anterior margin straight and posterior slightly curved. In contrast to other pelomedusoids, UF/IGM 72 only has seven pairs of costal bones. The neural series is completely absent, as in *Bairdemys*

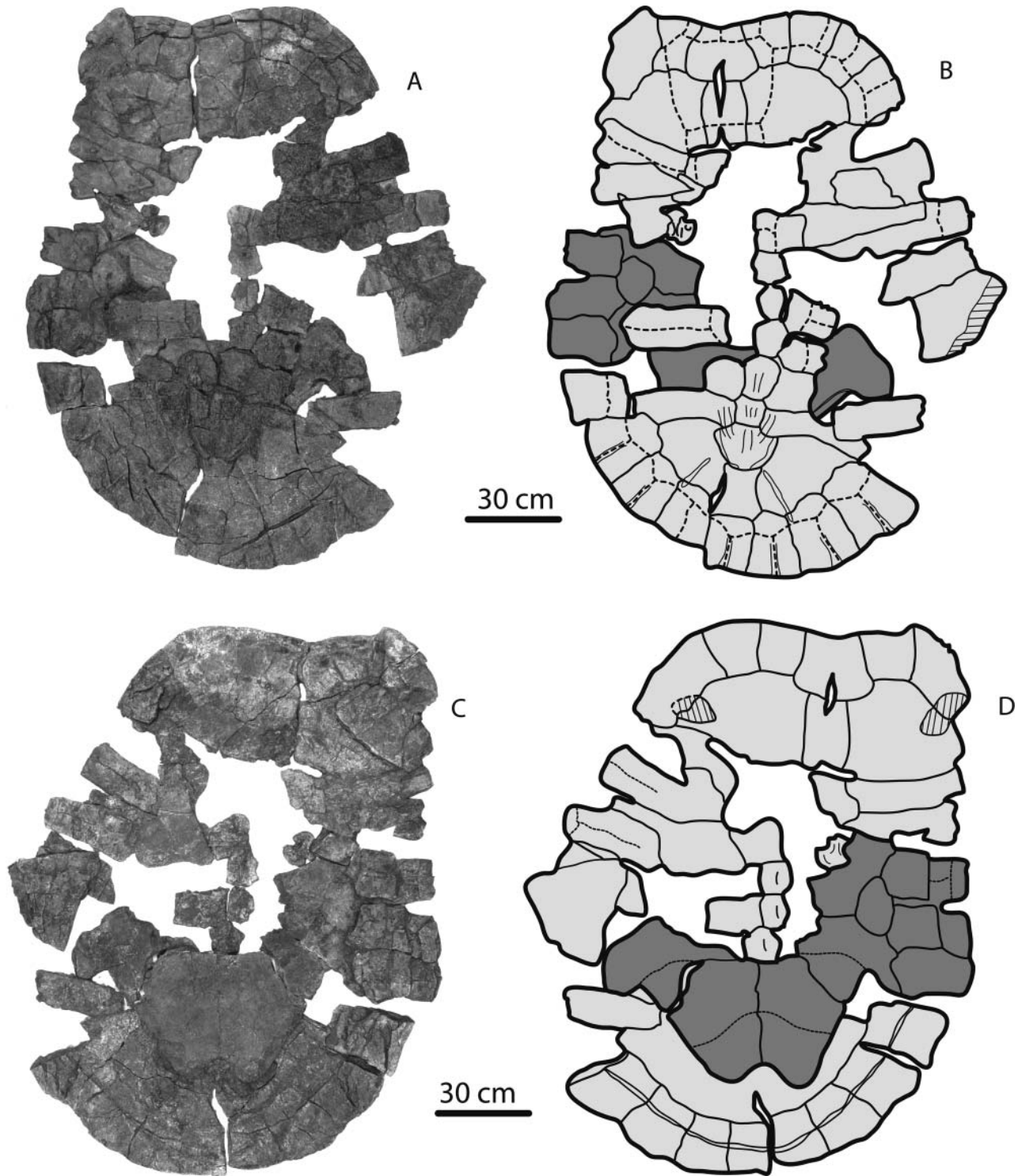


Figure 4. *Pelomedusoides incertae sedis* Taxon A, UF/IGM 71. **A, B**, shell in dorsal view; **C, D**, shell in ventral view. Dark grey represents elements of the plastron.

venezuelensis and most species of Chelidae. Suprapygals 1 is triangular in shape. The cervical scale is absent as in other pelomedusoids. Vertebral scale 1 has a trapezoidal shape and is considerably longer than wide, and larger

than the other four vertebral scales. All marginal scales are restricted to peripherals. On the ventral surface, both axillary buttresses are strongly developed medially and exteriorly projected onto peripheral 3. The plastron is slightly

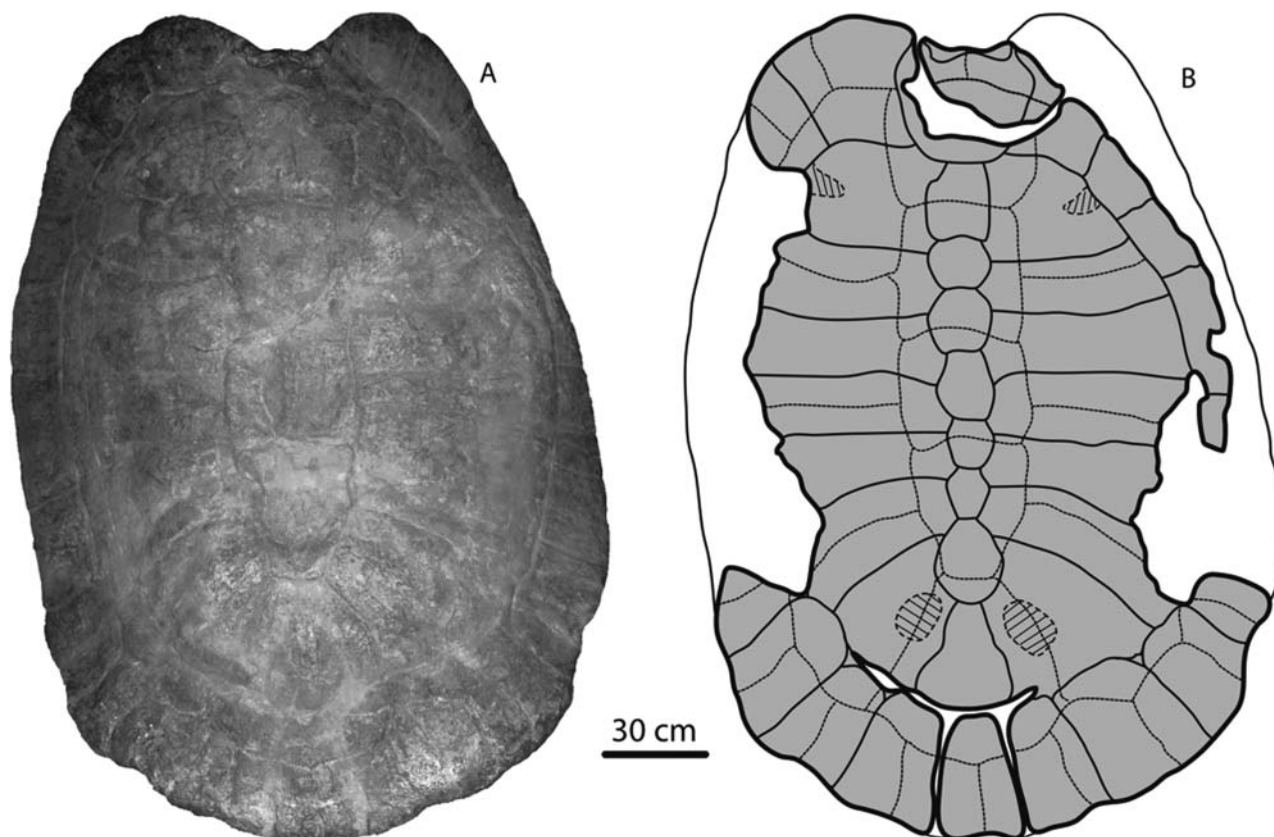


Figure 5. *Stupendemys geographicus* Wood, 1976, MCZ4376, holotype. **A, B,** carapace in dorsal view. Dark grey represents the original bone.

shorter than the carapace, with the posterior lobe shorter than the bridge length and slightly longer than the anterior lobe. The anal notch is a shallow, V-shaped incision. The mesoplastron is almost circular in shape as in other pelomedusoids. The entoplastron has a diamond shape and is slightly wider than long. The gular scales are small, triangular in shape and restricted to the epiplastron. The intergular has a pentagonal shape. It contacts the pectorals posteriorly, completely separating the humerals, as in some bothremydids, which are triangular in shape and lack a projection over the hyoplastra. On the dorsal surface, the ischiac and pubis scars are well defined on the xiphiplastra. The pubis scar is oval in shape and located at the mid-anterior portion of the xiphiplastron. The ischiac scar is triangular and extends far medially.

UF/IGM 73 (Fig. 6G–J) is a partially preserved articulated shell, with evidence of crushing and fragmentation. As in UF/IGM 72 the neural series is completely absent. The pygal is trapezoidal in shape, as can be observed on the ventral surface. The right posterior portion of the plastron is preserved, exhibiting a shallow V-shaped anal notch. The abdominofemoral and femoroanal sulci are almost parallel to each other. The left hypoplastron shows on its anterolateral portion the space for the mesoplastron, indicating

that the shape of this element was similar to that in other pelomedusoids.

UF/IGM 74 (Fig. 6K–P) is a small (15 cm long, 13 cm wide) articulated and crushed shell, showing the diagnostic absence of the neural series. The carapace and plastron are marked by a series of shallow circular holes arranged in an almost symmetrical pattern (Fig. 6O, P), which we interpret as bite marks. No evidence of healing can be observed.

UF/IGM 75 (Fig. 6Q, R) is constituted by only two elements: the nuchal and the right costal 1. With a maximum estimated length of 10 cm, this is the smallest individual turtle so far collected from the Cerrejón Formation. The nuchal is pentagonal in shape, lacking cervical scales. The medial margin of the costal 1 is straight, being parallel to the midline of the shell, indicating the absence of at least neural 1. On the ventral surface, the axillary scar is clearly outlined, indicating also that the axillary buttress projects laterally onto peripheral 3.

Phylogenetic analysis

We performed multiple analyses to test the phylogenetic position of *Carbonemys cofrinii*. Parsimony analyses were

conducted using a morphological dataset and a combined morphological and molecular dataset. In order to explore the possibility that Pelomedusoides shell taxon A represents the shell of *Carbonemys coffrinii*, we also undertook a set of analyses combining codings from the *Carbonemys coffrinii* holotype skull and UF/IGM 71 into a single terminal. Finally, we conducted a set of analyses including Pelomedusoides shell taxon A as a separate terminal to explore the possibility that UF/IGM 71 belongs to a distinct species.

All taxa were coded at the species level. A total of 30 species from Pelomedusoides were sampled in addition to *Carbonemys coffrinii*; *Chelus fimbriata* and *Phrynops geoffroanus* were chosen as outgroups. The fossil species *Podocnemis bassleri* was identified as a wildcard taxon (Nixon & Wheeler 1992), contributing to a large polytomy among the modern species of *Podocnemis* in a preliminary analysis of the combined dataset. This species is a taxonomic equivalent of several extant species of *Podocnemis* based on available codings, and so can be excluded using safe taxonomic deletion (Wilkinson 1995) without altering the relationships of the remaining taxa. We therefore conducted the final round of combined analyses discussed below with *Podocnemis bassleri* excluded.

The morphological dataset includes 46 characters and is presented in Appendix 1 (Online Supplementary Material). All morphological characters were equally weighted and unordered. Multistate characters were treated as polymorphic.

Molecular sequence data generated by previous studies were included in the combined analysis for the extant taxa *Chelus fimbriata*, *Pelomedusa subrufa*, *Erymnochelys madagascariensis*, *Peltocephalus dumerilianus* and the six extant species of *Podocnemis*. Accession numbers and original citations are provided in Appendix 2 (Online Supplementary Material). Sequences from cytochrome b, 12S RNA (12S), NADH dehydrogenase 4 (ND4), recombination activating genes 1 and 2 (RAG-1, RAG-2), intron 1 of RNA-fingerprint protein 35 (R35), and neurotrophin-3 (NT3) were downloaded from GenBank and aligned in Clustal X (Thompson *et al.* 1997). Alignments were manually inspected and adjusted in MacClade 4.08 (Maddison & Maddison 1992), and then concatenated. Molecular and morphological characters were weighed equally in the combined analysis.

All analyses were conducted in PAUP 4.0b10 (Swofford 2002), using a heuristic search strategy with 10 000 random taxon addition replicates and TBR branch swapping. Bootstrap values were calculated from 1000 replicates using the same settings as the primary search and Decay (Bremer) Indices were obtained using TreeRot v. 2 (Sorenson & Franzoza 2007) to estimate statistical support for nodes. Tree lengths for alternative phylogenetic hypotheses were explored using Mesquite v. 2.72 (Maddison & Maddison 2009).

Results

Analysis of the morphological dataset yielded four most parsimonious trees (total length (TL) = 81 steps; consistency index (CI) = 0.76; retention index (RI) = 0.90; re-scaled consistency index (RC) = 0.69). The strict consensus of these trees is shown in Fig. 7A. Analysis of the combined dataset also yielded four most parsimonious trees (TL = 2901 steps; CI = 0.71; RI = 0.50; RC = 0.37), but these trees differ from the morphological trees in the placement of several key taxa, as discussed below. The strict consensus of the most parsimonious trees from the combined analysis is shown in Fig. 7B. When shell character codings from UF/IGM 71 were incorporated into the *Carbonemys coffrinii* terminal, 102 most parsimonious trees (TL = 81; CI = 0.76; RI = 0.90; RC = 0.68) were recovered in the morphology-only analysis and four most parsimonious trees (TL = 2901; CI = 0.71; RI = 0.51; RC = 0.37) were recovered in the combined analysis. The topologies of the strict consensus trees from these two analyses were identical to those resulting from the counterpart morphology-only and combined analyses using only codings from the holotype skull for *Carbonemys coffrinii*. Finally, the analysis including Pelomedusoides shell taxon A as a separate terminal resulted in 102 most parsimonious trees (TL = 81 steps; CI = 0.76; RI = 0.90; RC = 0.69) using the morphological dataset and 139 most parsimonious trees (TL = 2901 steps; CI = 0.71; RI = 0.52; RC = 0.37) using the combined dataset. A near complete loss of resolution is observed in the strict consensus trees from both analyses, with almost every taxon within Podocnemoidae collapsed into a polytomy.

Discussion

The phylogenetic position of *Carbonemys coffrinii*

Results from the morphology-based phylogenetic analysis placed *Carbonemys coffrinii* as a member of Erymnochelyinae (Fig. 7A), which comprises two subclades, one uniting the extant monotypic *Erymnochelys madagascariensis* and *Peltocephalus dumerilianus*, and the other uniting a large set of fossil taxa (including *C. coffrinii*). Synapomorphies of Erymnochelyinae present in *C. coffrinii* include: prefrontals completely covering the apertura narium externa and ending in a straight to convex edge (Character 5); a very deep temporal emargination (Character 6); and a very wide prefrontal bone at the interorbital space (Character 8). Within Erymnochelyinae, *C. coffrinii* forms a subclade together with *Dacquemys paleomorpha*, *Shweboemys antiqua*, *Stereogenys cromeri* and *Bairdemys* spp., united by the absences of a foramen palatinum posterius (Character 27). Presence of this foramen in *B. harsteini*, *B. venezuelensis*

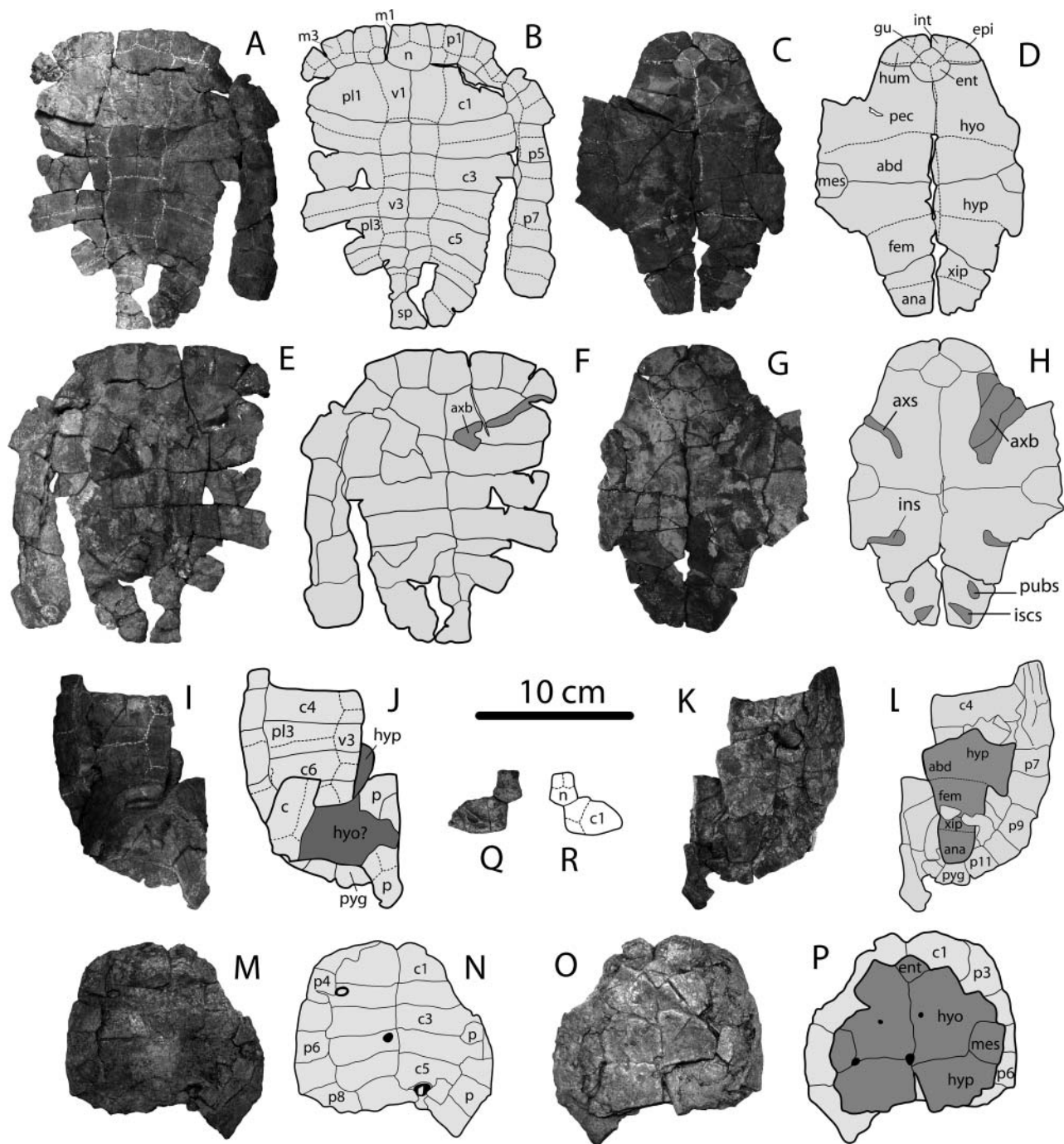


Figure 6. *Pelomedusoides incertae sedis* Taxon B. **A, B**, carapace in dorsal view, UF/IGM 72; **C, D**, plastron in ventral view, UF/IGM 72; **E, F**, carapace in ventral view, UF/IGM 72; **G, H**, plastron in dorsal view, UF/IGM 72; **I, J**, partial shell in dorsal view, plastral elements in dark grey, UF/IGM 73; **K, L**, partial shell in ventral view, plastral elements in dark grey, UF/IGM 73; **M, N**, nearly complete shell in dorsal view, black spots represent crocodile bite marks, UF/IGM 74; **O, P**, nearly complete shell in ventral view, black spots represent crocodile bite marks, plastral elements in dark grey, UF/IGM 74; **Q**, the smallest turtle from the Cerrejón Formation, nuchal and costal 1 in ventral view, UF/IGM 75; **R**, nuchal and costal 1 in dorsal view, UF/IGM 75. Abbreviations: abd, abdominal scale; axb, axillary buttress; axs, axillary scar; c, costal; ent, entoplastron; epi, epiplastron; fem, femoral; gu, gular; hum, humeral; hyo, hyoplastron; hyp, hypoplastron; ins, inguinal scar; int, intergular; iscs, ischial scar; m, marginal; mes, mesoplastron; n, nuchal; p, peripheral; pec, pectoral; pl, pleural; pubs, pubis scar; pyg, pygal; sp, suprapygal; v, vertebral; xip, xiphoplastron.

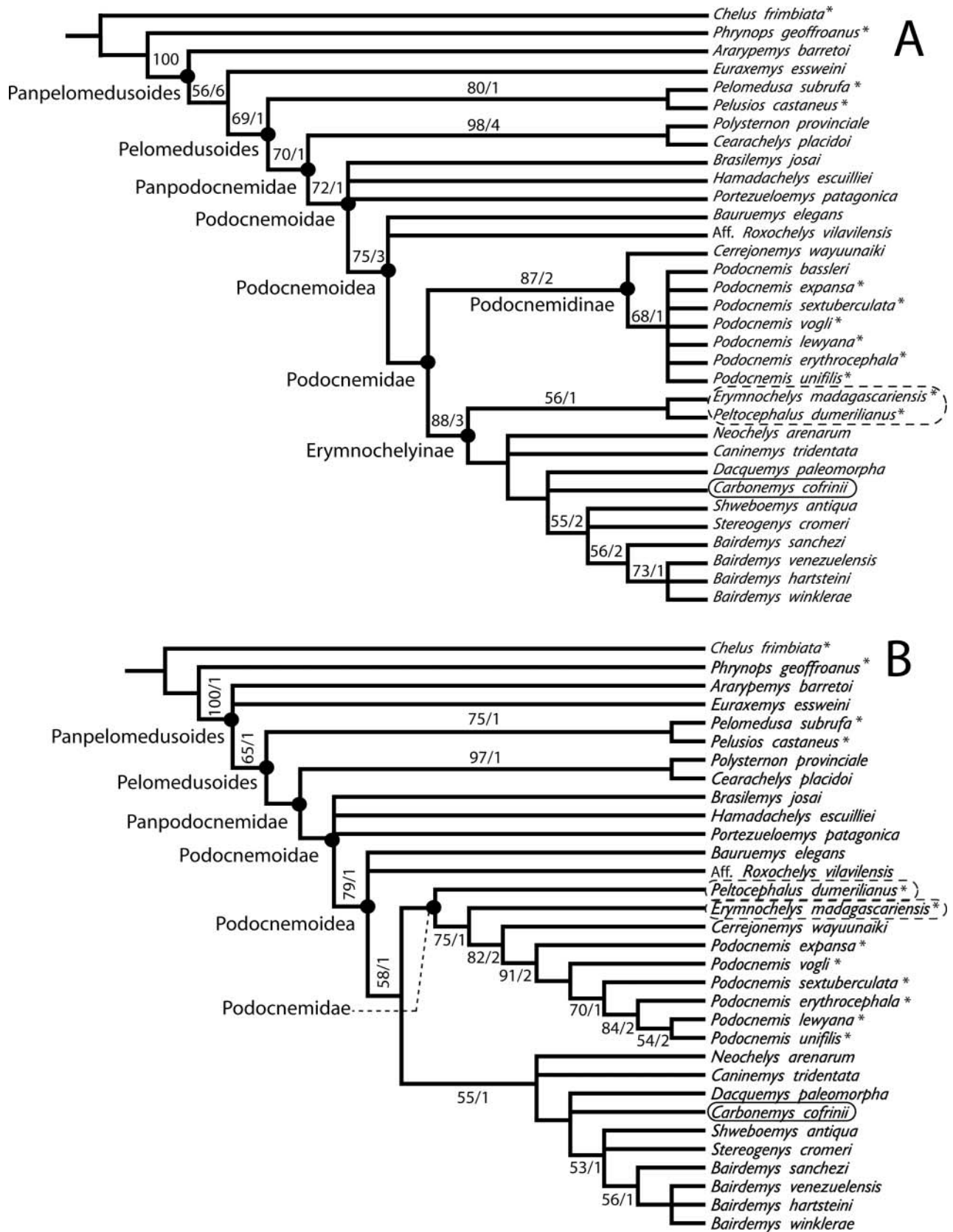


Figure 7. Strict consensus cladogram showing the phylogenetic relationships between panpelomedusoid turtles recovered in the current analysis. **A**, cladogram obtained based on morphological characters only. Bootstrap support values (left number before dash) and Bremer decay indices (right numbers after dash) are indicated above the branch they pertain to. **B**, cladogram obtained from the combination of morphological and molecular data. For both cladograms extant taxa are indicated with an asterisk. Bootstrap support values obtained from 1000 replicates.

and *B. winklerae* is interpreted as a reversal (Cadena *et al.* 2010).

In contrast, the combined molecular–morphological analysis (Fig. 7B) resolved *Peltocephalus dumerilianus* and *Erymnochelys madagascariensis* as successive sister taxa to Podocnemidinae, in agreement with previous molecular studies (Noonan & Chippindale 2006; Vargas-Ramirez *et al.* 2008). The collapse of the *P. dumerilianus* and *E. madagascariensis* clade is not surprising, as only a single synapomorphy supports this dyad in the morphological analysis. All fossil taxa recovered as part of the Erymnochelyinae in the morphological analysis instead form the sister taxon of Podocnemididae (*P. dumerilianus* + (*E. madagascariensis* + Podocnemidinae)). This shift is crucial, as it implies that the fossil taxa *Carbonemys cofrinii*, *Neochelys* spp., *Caninemys tridentata*, *Shweboemys* spp., *Stereogenys cromeri* and *Bairdemys* spp. all lie outside the crown radiation of Podocnemididae. However, the topology recovered in the morphology-only analysis is only two steps longer than the most parsimonious tree recovered in the combined analysis.

The position of *Carbonemys cofrinii* does not shift when codings from the large shell (UF/IGM 71) recovered at the same locality are added, so it remains plausible that *Carbonemys cofrinii* and Pelomedusoides shell taxon A represent the same species. Including UF/IGM 71 as a separate taxon does not result in this shell specimen forming a clade with the *Carbonemys cofrinii* holotype skull, but this may be attributed to the complete lack of overlapping material. Recently, (Gaffney *et al.* 2011) in absence of examination of the holotype, attributed *Cerrejonemys wayuunaiki* Cadena *et al.* 2010 as dubious taxa, however we dispute this attribution and consider that there is strong evidence to support *C. wayuunaiki* as podocnemid: presence of a cavum pterygoidei and the horse-saddle posterior condyle of cervical vertebra, and also as sister taxon to *Podocnemis* genus: small postorbital allowing a jugalparietal contact.

Relationships within the genus *Podocnemis* are fully resolved in the results of the combined analysis, in contrast to the results of the morphological analysis where the six extant species are collapsed into a polytomy. We note that the extant species remain collapsed in a polytomy when *P. bassleri* is excluded from the morphological analysis, indicating that the lack of resolution is a result of weak or conflicting phylogenetic signal in the morphological dataset for *Podocnemis* spp. rather than the effects of a wildcard taxon. Relationships within *Podocnemis* spp. are nearly identical to those recovered by Vargas-Ramirez *et al.* (2008, fig. 4), with the sole difference that our analysis resolved *P. unifilis* as the sister taxa of *P. lewyana*, rather than *P. erythrocephala*.

Regardless of whether the morphological or combined tree is preferred, Late Cretaceous fossils of turtles closely related to *Erymnochelys madagascariensis* support the splitting of the lineages leading to the three extant genera of

Podocnemididae (*Peltocephalus*, *Erymnochelys* and *Podocnemis*) by at least 65 million years ago (Gaffney & Forster 2003). This is a minimum estimate, and given the large gap spanning the Late Jurassic–Late Cretaceous interval in the fossil record of Madagascar (Krause *et al.* 1999), and the fact that no fossil representatives of the putatively basal *Peltocephalus* lineage have yet been discovered, a significantly older date is quite plausible. Indeed, the basal divergence in the crown Podocnemididae was estimated to have occurred around 85 Ma based on divergence dating analyses (Vargas-Ramirez *et al.* 2008).

Relationships among modern podocnemids are far from resolved. While morphological and molecular data yield very different results, neither is overwhelmingly supported. Future contributions, for example the sequencing of more genes for the modern species and the discovery of new fossil taxa, may add new information supporting any of the two phylogenetic hypotheses described here. Previous combined analyses have demonstrated that the phylogenetic positions of fossil taxa may be strongly affected by the inclusion of molecular data (Gatesy *et al.* 2003; O’Leary & Gatesy 2008). The present study reinforces the importance of considering both morphological and molecular data when studying clades with both fossil and extant representatives. Molecular data affect the relationships of the extant taxa sufficiently to impact the placement of many fossil taxa by changing the polarity of some morphological characters at key nodes. Morphological data, of course, are necessary to incorporate any fossil taxa into the framework of pelomedusoid phylogeny.

Pelomedusoides incertae sedis from Cerrejón Formation

The large shell (UF/IGM 71) described here as Pelomedusoides shell taxon A resembles *Stupendemys geographicus* from the Late Miocene of Venezuela in several characteristics. Both retain primitive character states, including the presence of a neural series completely separating the posterior costals as in basal panpleurodires (platychelyids) and panpelomedusoids (*Araripemys barretoii*), as well as the presence of two suprapygals bones, also characteristic of platychelyids (Cadena & Gaffney 2005). Besides these discrete morphological similarities, Pelomedusoides shell taxon A and *S. geographicus* also share a very large body size and similar proportions between the carapace and the plastron (approximately 2:1). It is very plausible that these two large pelomedusoids share a common ancestor, forming a clade that should have split from other pelomedusoids during the late Cretaceous or early Palaeocene, at the same time as the split between Erymnochelyinae and Podocnemidinae (Romano & Azevedo 2006).

Taxonomic uncertainty related to skeletal non-overlap between fossil ‘skull taxa’ and ‘shell taxa’ is a recurring problem in turtle palaeontology (e.g. Gaffney 1972; Danilov & Parham 2005; Parham 2005; Lyson & Joyce 2010). It is

plausible that the shell of Pelomedusoides shell taxon A belongs to *Carbonemys cofrinii*. This hypothesis is consistent with the relative size of the fossils and the fact that both were found at the same stratigraphical horizon (Fig. 1B), separated by a linear distance of only 200 m. Incorporating codings from Pelomedusoides shell taxon A into the *Carbonemys cofrinii* terminal does not alter the phylogenetic position of the species, indicating there is little or no conflict between the phylogenetic signal in the skull and shell character data. Nonetheless, we prefer to proceed cautiously and do not refer UF/IGM 71 to *Carbonemys cofrinii* at this time in order to avoid potential creation of a fossil chimera. Ultimately the resolution of this issue must await future discoveries of associated skull and shell material.

Pelomedusoides shell taxon B shares shell character states with the podocnemid *Bairdemys venezuelensis* from the late Miocene of Venezuela, as well as many chelids which also lack the neural series (e.g. *Platemys platycephala* and *Emydura macquarii*). Reduction or complete loss of the neural series has been attributed to loss of mesenchymal–epithelial interaction and/or the lack of muscular interaction (Scheyer *et al.* 2008). Adaptive significance and functional implications of the loss of the neural

series remain speculative. Hypotheses include increased overall shell strength, reduction of asymmetrical tensional stresses on the shell of powerful swimmers, and reduction of forces accompanying lateral thrust feeding in long-necked forms (Pritchard 1988). The fossils described here constitute the earliest evidence of complete reduction of neurals in pleurodiran turtles. Based on the evidence from crocodile bite marks on the shell of specimen UF/IGM 74 (Fig. 6O, P), it is clear these turtles lived alongside crocodylomorph predators. We hypothesize that loss of neurals may have helped in the locomotion of these small turtles, potentially releasing tensional stress as proposed by Pritchard (1988) and improving the swimming speed required to escape from predators. Pelomedusoides shell taxon B has pectoral scales that contact epiplastra, a character considered as diagnostic of Podocnemidae by (Gaffney *et al.* 2011). However, based on the examination of important number of extant podocnemids (Online Supplementary Material) we conclude that, this character is very variable within podocnemids, particularly in *Peltocephalus dumerilianus*, *Podocnemis erythrocephala*, and *P. lewyana*, which exhibited pectorals restricted to hypoplastra, but covering the posterior portion of the entoplastron as in most bothremydids.

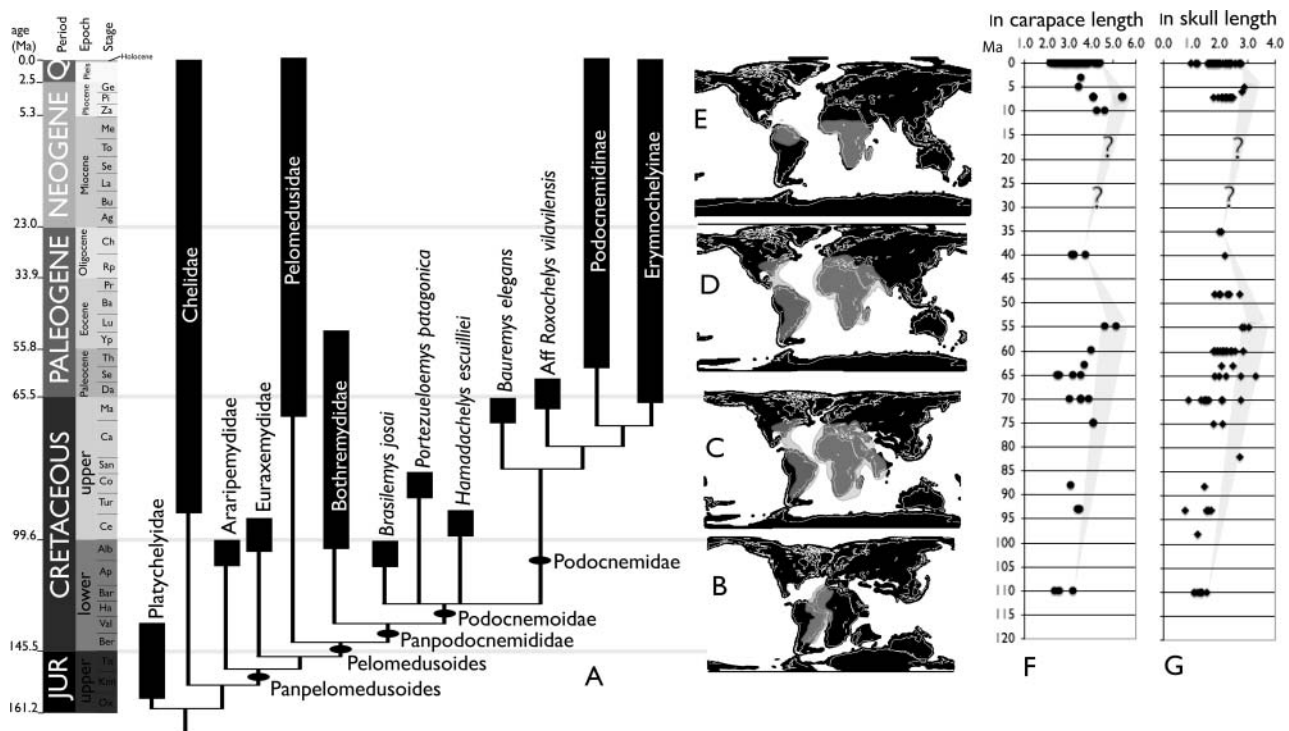


Figure 8. Panpelomedusoides phylogeny in the context of Mesozoic–Cenozoic biogeographical distribution and body size tendency. **A**, temporal distribution of clades using the geological timescale of Ogg *et al.* (2008). **B–E**, Mesozoic–Cenozoic distribution of panpelomedusoids shown in grey, superimposed on plate tectonic reconstructions (downloaded from the Paleobiology Database on 20 May 2010) for: **B**, Early Cretaceous; **C**, Late Cretaceous–Palaeocene; **D**, Neogene; and **E**, the present day. **F**, **G**, plot of ln length of Mesozoic–Cenozoic panpelomedusoid skull (**F**) and carapace (**G**) lengths versus time (see Online Supplementary Material for primary data).

Body size implications of Cerrejón turtles

The development of large body size has been explained by latitudinal gradient variations (Bergman's Rule; e.g. Watt *et al.* 2010), directional evolutionary tendencies (Cope's Rule), and temperature and metabolic rate (Head *et al.* 2009). Very large body size has evolved multiple times in different turtle lineages, including the Late Cretaceous marine turtles *Archelon ischyros* (possibly up to 4 m maximum length; Wieland 1896) and *Protostega gigas* (3 m maximum length; Cope 1872), the Late Cretaceous brackish bothremydid turtle *Nigeremys gigantea* (20 cm skull length; Bergounioux & Crozel 1968; Gaffney *et al.* 2006), and the giant freshwater podocnemid turtles from the Late Miocene–Pliocene of tropical South America, including *Stupendemys geographicus*, *Stupendemys souzai* and *Caninemys tridentata* (Meylan *et al.* 2009). Several extant turtles reach comparable sizes as well, including the chelonoid sea turtle *Dermochelys coriacea* (2 m maximum length; Wood *et al.* 1996), the giant land tortoises of the Galapagos and Aldabra islands, and the extant Chinese soft shell turtle *Rafetus swinhoei* (1 m maximum length; Meylan & Webb 1988). Turtles from Cerrejón can now be added to this roster. UF/IGM 41 constitutes the largest Palaeocene turtle ever, and the second largest pleurodiran after *Stupendemys geographicus*.

In order to take a first look at body size trends in Panpelomedusoides, we collected measurements of 131 skulls and 80 shells including fossil and extant taxa (Online Supplementary Material). Length and width measures were log-transformed in order to reduce the positive skew of the length distribution (Moen 2006). A plot of the carapace and skull length versus time (Fig. 8F, G) shows a marked trend in increasing size between the Early Cretaceous and Palaeocene. During the late Eocene a decrease in size for both carapace and skull is evident. Whether this tendency continued during the Oligocene and Early Miocene is unknown due to a large gap in the fossil record. Late Miocene and early Pliocene fossils increase in size again, reaching the maximum sizes for the Cenozoic with *Stupendemys* spp. The last 5 million years are also marked by a trend of decreasing maximum body size, with extant representatives of Pelomedusoides reaching at maximum 85 cm carapace length in *Podocnemis expansa* (Online Supplementary Material).

Climate change, particularly environmental temperature, is considered one of the key factors driving trends of increasing maximum body size in poikilotherms (Makarieva *et al.* 2005; Head *et al.* 2009). However, the pattern of body size in panpelomedusoids does not seem to match with the trends in Cretaceous–Cenozoic temperatures (Jenkyns *et al.* 2004; Zachos *et al.* 2008). While temperatures in the Cretaceous were warmer than in the Cenozoic, a corresponding increase in body size is not apparent in pelomedusoid turtles. The largest shell sizes are found in the Late Miocene, an interval of cooler climate

than the Palaeocene or Late Eocene, when smaller species occur. It is thus probable that other factors, such as habitat area and ecological interactions, drove Cenozoic shifts in body size in panpelomedusoid turtles.

Biogeographical implications of the Cerrejón turtles

Cerrejón turtle fossils demonstrate that at least two major subclades of Podocnemidae were already in place in the neotropics by the Early Cenozoic. This indicates that dispersal of pelomedusoids to this region likely occurred by the Late Cretaceous or Early Palaeocene (Fig. 8C) (Romano & Azevedo 2006; Cadena *et al.* 2010). Pelomedusoids enjoyed a wide, relatively stable distribution during the Palaeogene (Fig. 8D) but suffered a major range retraction over the Miocene to present day interval, resulting in a present distribution limited to sub-Saharan Africa, Madagascar and northern South America (Fig. 8E).

Acknowledgements

Funding for this project came from the Smithsonian Paleobiology Endowment Fund, the Florida Museum of Natural History, National Science Foundation grant DEB-0733725, Florida Museum of Natural History Miss Lucy Dickinson Fellowship, the Fondo para la Investigación de Ciencia y Tecnología Banco de la República de Colombia, the Unrestricted Endowments Smithsonian Institution Grants, and Carbones del Cerrejón LLC. We thank A. Rincon for collecting the skull of *Carbonemys cofrinii*, and L. Teicher, F. Chavez, C. Montes, G. Hernandez and the geology team at Cerrejón SA for logistical support during fieldwork. J. Head provided useful comments on the preliminary draft that improved this paper. Thanks for access to collections go to Dr F. de Lapparent de Broin (Muséum National d'Histoire Naturelle, Paris); Dr E. Gaffney and C. Mehling (Fossil Amphibians, Reptiles, and Birds Collections, Division of Paleontology, American Museum of Natural History, New York); and C. Weisel (Museum of Comparative Zoology, Harvard University, Boston). Special thanks go to F. Herrera, A. Hastings, A. Rincon, S. Moron, L. Meza, I. Gutierrez, G. Bayona, C. Sanchez, T. Gaona, S. Wing, D. Dilcher, the Colombian Petroleum Institute-Ecopetrol SA, Smithsonian Tropical Research Institute, and the Florida Museum of Natural History.

References

- Batsch, A. C. 1788. *Versuch einer Anleitung, zur Kenntniß und Geschichte der Thiere und Mineralien*. Akademische Buchhandlung, Jena, 528 pp.
- Bayona, G., Jaramillo, C. A., Rueda, M. J., Pardo, A., Christie, A. & Hernandez, G. 2004. Important paleotectonic and

- paleogeographic considerations of the late Paleocene in the Northernmost Andes as constrained by Paleogene rocks in the Cerrejón Coal Mine, Guajira, Colombia. *III Convención Técnica ACGGP. Lainversion en el conocimiento geológico*. P4, CD-ROM, ACGGP, Bogotá.
- Bergounioux, F. M. & Crouzel F.** 1968. Deux tortues fossiles d'Afrique. *Bulletin de la Société d'Histoire Naturelle de Toulouse*, **104**, 179–186.
- Cadena, E. A. & Gaffney E. S.** 2005. Notoemys zapatocaensis, a new side-necked turtle (Pleurodira:Platycheilyidae) from the Early Cretaceous of Colombia. *American Museum Novitates*, **3470**, 1–19.
- Cadena, E. A., Bloch, J. I. & Jaramillo, C. A.** 2010. New podocnemid turtle (Testudines: Pleurodira) from the Middle–Upper Palaeocene of South America. *Journal of Vertebrate Paleontology*, **30**, 367–382.
- Cope, E. D.** 1864. On the limits and relations of the Raniformes. *Proceedings of the Academy of Natural Sciences of Philadelphia*, **16**, 181–183.
- Cope, E. D.** 1872. A description of the genus Protostega. *Proceedings of the Academy of Natural Sciences of Philadelphia*, **40**, 422–433.
- Danilov, I. G. & Parham, J. F.** 2005. A reassessment of the referral of an isolated skull from the Late Cretaceous of Uzbekistan to the stem-testudinoid turtle genus Lindholmemys. *Journal of Vertebrate Paleontology*, **25**, 784–779.
- De la Fuente, M.** 2003. Two new pleurodiran turtles from the Portezuelo Formation (Upper Cretaceous) of Northern Patagonia, Argentina. *Journal of Paleontology*, **77**, 559–575.
- França, M. A & Langer, M. C.** 2006. Phylogenetic relationships of the Bauru Group turtles (late Cretaceous of South Central Brazil). *Revista Brasileira de Paleontologia*, **9**, 365–373.
- Gaffney, E. S.** 1972. The systematics of the North American family Baenidae (Reptilia, Cryptodira). *Bulletin of the American Museum of Natural History*, **147**, 241–320.
- Gaffney, E. S. & Forster, C. M.** 2003. Side-necked turtle lower jaws (Podocnemidae, Bothremydidae) from the Late Cretaceous Maevarano Formation of Madagascar. *American Museum Novitates*, **3397**, 1–13.
- Gaffney, E. S., DeBlieux, D., Simons, E., Sánchez-Villagra, M. & Meylan, P. A.** 2002. Redescription of the skull of Dacquemys Williams, 1954, a podocnemid sidenecked turtle from the Late Eocene of Egypt. *American Museum Novitates*, **3372**, 1–16.
- Gaffney, E. S., Tong, H. & Meylan, P. A.** 2006. Evolution of the side-necked turtles: the families Bothremydidae, Euraxemydidae, and Araripemydidae. *Bulletin of the American Museum of Natural History*, **300**, 1–698.
- Gaffney, E. S., Meylan, P. A., Wood, R. C., Simons, E. & De Almeida-Campos, D.** 2011. Evolution of the side-necked turtles: The family Podocnemidae. *Bulletin of the American Museum of Natural History*, **350**, 1–37.
- Gatesy, J., Amato, G., Norell, M., DeSalle, R. & Hayashi, C.** 2003. Combined support for wholesale taxic atavism in gavioline crocodylians. *Systematic Biology*, **52**, 403–422.
- Hastings, A. K., Bloch, J. I., Cadena, E. A. & Jaramillo, C. A.** 2010. A new small short-snouted dyrosaurid (Crocodylomorpha, Mesoeucrocodylia) from the Palaeocene of Northeastern Colombia. *Journal of Vertebrate Paleontology*, **30**, 139–162.
- Head, J. J., Bloch, J. I., Hastings, A. K., Bourque, J. R., Cadena, E. A., Herrera, F. A., Polly, D. P. & Jaramillo, C. A.** 2009. Giant boid snake from the Palaeocene neotropics reveals hotter past equatorial temperatures. *Nature*, **457**, 715–718.
- Jaramillo, C. A., Bayona, G., Pardo, A., Rueda, M. J., Harrington, G. & Mora, G.** 2007. Palynology of the Upper Palaeocene Cerrejón Formation, Northern Colombia. *Palynology*, **31**, 153–189.
- Jenkyns, H. C., Forster, A., Schouten, S. & Sinninghe Damste, J. S.** 2004. High temperatures in the Late Cretaceous Arctic Ocean. *Nature*, **432**, 888–892.
- Joyce, W. G.** 2007. Phylogenetic relationships of Mesozoic turtles. *Bulletin of Peabody Museum of Natural History*, **48**, 1–100.
- Joyce, W. G., Parham, J. F. & Gauthier, J.** 2004. Developing a protocol for the conversion of rank-based taxon names to phylogenetically defined clade names, as exemplified by turtles. *Journal of Paleontology*, **78**, 989–1013.
- Krause, D. W., Rogers, R. R., Forster, C. A., Hartman, J. H., Buckley, G. A. & Sampson, S. D.** 1999. The Late Cretaceous vertebrate fauna of Madagascar: implications for Gondwanan palaeobiogeography. *GSA Today*, **9**, 2–7.
- Lapparent de Broin, F.** 2000. The oldest pre-Podocnemid turtle (Chelonii, Pleurodira), from the Early Cretaceous, Ceará state, Brasil, and its environment. *Treballs del Museu de Geologia de Barcelona*, **9**, 43–95.
- Lapparent de Broin, F. de, Murelaga Bereikua, X. & Codrea, V.** 2004. Presence of Dortokidae (Chelonii, Pleurodira) in the earliest Tertiary of the Jibou Formation, Romania: paleobiogeographical implications. *Acta Paleontologica Romaniaae*, **4**, 20–21.
- Lapparent de Broin, F., De La Fuente, M. & Fernandez, M.** 2007. Notoemys laticentralis (Chelonii, Pleurodira), Late Jurassic of Argentina: new examination of the anatomical structures and comparisons. *Revue de Paléobiologie*, **26**, 99–136.
- Lyson, T. R. & Joyce, W. G.** 2010. A new baenid turtle from the Late Cretaceous (Maastrichtian) Hell Creek Formation of North Dakota and a preliminary taxonomic revision of Cretaceous Baenidae. *Journal of Vertebrate Paleontology*, **30**, 394–402.
- Maddison, W. P. & Maddison, D. R.** 1992. *MacClade: analysis of phylogeny and character evolution, Version 4.08*. Sinauer Associates, Sunderland.
- Maddison, W. P. & Maddison, D. R.** 2009. *Mesquite: a modular system for evolutionary analysis. Version 2.72* [updated at <http://mesquiteproject.org>, accessed 29 April 2010].
- Makarieva, A. M., Gorshkov, V. G. & Li, L.** 2005. Temperature-associated upper limits to body size in terrestrial poikilotherms. *Oikos*, **111**, 425–436.
- Meylan, P. A. & Webb, R.** 1988. *Rafetus swinhoei* (Gray) 1873, a valid species of living soft-shelled turtle (family Trionychidae) from China. *Journal of Herpetology*, **22**, 118–119.
- Meylan, P. A., Gaffney, E. S. & De Almeida Campos, D. L.** 2009. *Caninemys*, a new side-necked turtle (Pelomedusoides: Podocnemidae) from the Miocene of Brazil. *American Museum Novitates*, **2639**, 1–26.
- Moen, D. S.** 2006. Cope's rule in cryptodiran turtles: do the body sizes of extant species reflect a trend of phyletic size increase?. *Journal of Evolutionary Biology*, **19**, 1210–1221.
- Nixon, B. P. & Wheeler, Q. D.** 1992. Extinction and the origin of species. Pp. 199–143 in M. J. Novacek & Q. D. Wheeler (eds) *Extinction and Phylogeny*. Columbia University Press, New York.
- Noonan, B. P. & Chippindale, P. T.** 2006. Vicariant origin of Malagasy reptiles supports Late Cretaceous Antarctic land bridge. *American Naturalist*, **168**, 730–741.
- Ogg, J. G., Ogg, G. & Gradsteine, F.** 2008. *The concise Geologic Time Scale*. Cambridge University Press, Cambridge, UK.

- O'Leary, M. A. & Gatesy, J.** 2008. Impact of increased character sampling on the phylogeny of Cetartiodactyla (Mammalia): combined analysis including fossils. *Cladistics*, **24**, 397–442.
- Parham, J. F.** 2005. A reassessment of the referral of sea turtle skulls to the genus *Osteopygis* (Late Cretaceous, New Jersey, USA). *Journal of Vertebrate Paleontology*, **25**, 71–77.
- Pritchard, P.** 1988. A survey of neural bone variation among recent chelonian species, with functional interpretations. *Acta Zoologica Cracoviana*, **31**, 625–686.
- Romano, P. S. & Azevedo, S. A.** 2006. Are podocnemid turtles relicts of a spread Cretaceous ancestor? *South American Journal of Herpetology*, **1**, 175–184.
- Scheyer, T., Brullmann, B. & Sanchez-Villagra, M.** 2008. The ontogeny of the shell in side-necked turtles, with emphasis on the homologues of costal and neural bones. *Journal of Morphology*, **269**, 1008–1021.
- Sorenson, M. & Franzosa, E.** 2007. TreeRot Version 3 [updated at <http://people.bu.edu/msoren/TreeRot.html>, accessed 10 May 2010].
- Swofford, D.** 2002. *PAUP*. Phylogenetic Analysis Using Parsimony (*and other methods). Version 4.0b10*. Sinauer Associates, Sunderland.
- Thompson, J. D., Gibson, T. G., Plewniak, F., Jeanmougin, F. & Higgins, D. G.** 1997. The ClustalX Windows interface: flexible strategies for multiple sequence alignment aided by quality analysis tools. *Nucleic Acids Research*, **25**, 4876–4882.
- Vargas-Ramírez, M., Castaño-Mora, O. V. & Fritz, U.** 2008. Molecular phylogeny and divergence times of ancient South American and Malagasy river turtles (Testudines: Pleurodira: Podocnemidae). *Organisms, Diversity and Evolution*, **8**, 388–398.
- Watt, C., Mitchell, S. & Salewski, V.** 2010. Bergmann's rule; a concept cluster? *Oikos*, **119**, 89–100.
- Wieland, G.** 1896. Archelon ischyros: a new gigantic cryptodire testudinate from the Fort Pierre Cretaceous of South Dakota. *American Journal of Science, 4th Series*, **2**, 399–412.
- Wilkinson, M.** 1995. Coping with abundant missing entries in phylogenetic inference using parsimony. *Systematic Biology*, **44**, 501–514.
- Wood, R. C.** 1976. Stupendemys geographicus, the world's largest turtle. *Breviora*, **436**, 1–31.
- Wood, R. C., Johnson-Gove, J., Gaffney, R. & Maley, K.** 1996. Evolution and phylogeny of leatherback turtles (Dermochelyidae), with descriptions of new fossil taxa. *Chelonian Conservation Biology*, **2**, 266–286.
- Zachos, J. C., Dickens, G. R. & Zeebe, R. E.** 2008. An early Cenozoic perspective on greenhouse warming and carbon-cycle dynamics. *Nature*, **451**, 279–283.

Appendix 1: character list

Description of characters used in phylogenetic analysis. A NEXUS file containing the matrix is included in Supplementary Material 1. Characters were polarized with respect to *Chelus fimbriata* and *Phrynops Geoffroyanus*. Characters and codings are based on specimen examination and from the literature. Original citations for characters are indicated as follows unless otherwise noted: De La Fuente (2003) ('D'), Gaffney *et al.* (2006) ('G'), França & Langer (2006) ('FL'), Joyce (2007) ('J'), Meylan *et al.* (2009) ('M'), and Cadena *et al.* (2010) ('C').

Skull

1. Prefrontals meet on midline: absent (0); present (1). C2, J4, G4.
2. Quadratojugal: absent (0); present (1). C3, J16.
3. Squamosal parietal contact: present (0); absent (1). C4, G15, J11.
4. Quadratojugal parietal contact: absent (0); present (1). C5, M4.
5. Prefrontal, anterior overhang onto apertura narium externa: shaped by the nasals (0); by the prefrontals, covering a small portion of the posterior part of the apertura, ending in acute medial tip (1); by the prefrontals, completely covering the apertura, ending in a straight to convex edge (2). C7 and Gaffney *et al.* (2002).
6. Temporal emargination, secondary roofing of the fossa temporalis in dorsal view, not advanced and highly concave allowing the complete exposure of the otic chamber roof (0); medially advanced with posteriorly expanded posterolateral temporal emargination of the parietals and quadratojugal with concave margins, covering partially or almost totally the otic chamber roof (1); very advanced with convex to straight tapering margins completely covering the roof of the otic chamber (2). C6 and Lapparent de Broin (2000).
7. Prefrontal, interorbital sulcus at the sutural area between both prefrontals: absent (0); present (1). C9 and Lapparent de Broin (2000).
8. Prefrontal at the interorbital space: wide (0); narrow (1). C9, G5.
9. Prefrontal postorbital contact: absent (0); present (1). New character.
10. Parietal jugal contact: absent (0); present (1). C11, D3, M9.
11. Supraoccipital, crista supraoccipitalis: very short to absent (0); long, ventrally wider with uniform width from the anterior to the posterior aspect, ending in an acute tip in dorsal view (1); short, wider posteroventrally than anteroventrally, ending in a bulbous shape in dorsal view (2). In *Dacquemys* the crista supraoccipitalis is long, but is hidden dorsally by the large exposure of the supraoccipital at the posterior roof of the skull, coded as 1. C12, G80, J46.
12. Interparietal scale, anterior margin: anterior to the frontal parietal suture (0); posterior to the frontal parietal suture (1). C13.
13. Condylus occipitalis: formed by exoccipitalis and the basioccipital (0); formed only by exoccipitalis (1). C14, G84.
14. Quadrate basioccipital contact: absent (0); present (1). C15, G59.
15. Quadrate, cavum tympani, incisura columella auris: open without posterior bony restrictions (0); enclosed or slightly open by a quadrate no completed

closed posteriorly, Eustachian tube separated from stapes by bone (1); enclosed together with both stapes and Eustachian tube in the same oval dilated opening, posteriorly directed (2); Enclosed together with both stapes and Eustachian tube in the same oval dilated opening, downwards directed (3). C15, G52, and Lapparent de Broin *et al.* (2007). For the basal bothremydidae *Cearachelys*, the incisura is open and dilated including the Eustachian tube, but without the complete posterior closure of the quadrate as in Podocnemidae (Lapparent de Broin *et al.* 2007) plus *Hamadachelys*.

16. Quadrate, cavum tympani, fossa precolumellaris: deep (0); shallow (1); absent (2). C17, G55, G62, and Lapparent de Broin (2000).
17. Quadrate, ventral projection: very short, condylus mandibularis very close to the cavum tympani region (0); short, condylus mandibularis slightly separated from the cavum tympani region (1); long, condylus mandibularis considerably separated from the cavum tympani region (2). C18.
18. Cheek emargination, secondary lateral roofing of the fossa temporalis: fossa temporalis laterally exposed without secondary roofing (0); secondary roofing slightly advanced (1); secondary roofing moderately advanced by the descending of only the quadratojugal (2); secondary roofing moderately advanced by the descending of both the jugal and the quadratojugal (3); fossa temporalis completely roofed by the jugal, resulting in a contact between the quadrate and the jugal; occasionally with a small notch at the posterolateral margin of the jugal (4). C20, G39 and Lapparent de Broin *et al.* (2007)
19. One or two accessory ridges on the ventral surface of the premaxilla: absent (0); present (1). C21.
20. Vomer: present (0); absent (1). C22, M22, J27.
21. Basisoccipital: long (0); short (1). C23, G87, M39.
22. Opisthotic, processus paroccipitalis: small and flat, does not project beyond the squamosal (0); medially narrowed and elongated, projects beyond the squamosal ending in a prominent tip (1). C24, G102, and Lapparent de Broin *et al.* (2007).
23. Basisphenoid quadrate contact: absent (0); present (1). C25, G104.
24. Basisoccipital opisthotic contact: present (0); absent (1). C26, G89.
25. Pterygoid, pterygoid flange = pterygoid wings (Lapparent de Broin, 2000): absent to very short (0); moderately developed (1); well developed reaching the caudal margin of the quadrate ramus of the bone and projected ventrally (2). C28, FL14, and Lapparent de Broin (2000).
26. Pterygoid, cavum pterygoidei = fossa podocnemidoid of Lapparent de Broin, (2000): absent (0); shallow and slightly hidden anteromedially by the under-

lapping basisphenoid medially and the pterygoid laterally (1); deep and partially to totally covered by the pterygoid flange (posterolateral wings of the pterygoid) (2). C27, G68.

27. Palatine, foramen palatinum posterius: present (0); absent (1). C29, G48.
28. Palatine, second palate: absent (0); present (1). C30, M16.
29. Quadrate, condylus mandibularis shape: much wider than long, with anterior and posterior edges straight to concave making it shorter at midline (0); slightly wider than long in a 'kidney bean' shape, with anterior edge straight to concave and posterior edge convex (1). C31.
30. Exoccipital quadrate contact: absent (0); extensive (1); narrow (2). C32, G85.
31. Prootic quadrate contact: absent (0); present (1). C33, G95.
32. Prootic: exposed on the ventral view of the skull (0); completely covered ventrally by quadrate, basisphenoid, and pterygoid (1). G95.

Lower jaw

33. Dentary, fused symphysis: absent (0); present (1). C34
34. Dentary, internal angle between rami: acute, between 40° and 90° (0); obtuse, over 90° (1); very acute, less than 40° (2). C35.
35. Dentary, accessory ridges: absent (0); present (1). C39 and Gaffney & Forster (2003).
36. Dentary, narrow and elongated ridge, located in the medial margin on the ventral surface: absent (0); present (1). C40.

Cervical vertebrae

37. Ventral keel at the posterior condyle: protuberant (0); reduced almost absent (1). C41 and Lapparent de Broin (2000).
38. Posterior condyle of the sixth or previous cervical vertebrae in a horse-saddle shape, higher than wide: absent (0); present (1). C42 and Lapparent de Broin (2000).

Coracoid

39. Coracoid shape: slightly curved longitudinally and much wider distally (0); narrow, almost straight longitudinally and slightly wider distally (1). C43, G131.
40. Coracoid, dorsal longitudinal ridge: absent (0); present (1). C44.

Carapace

41. Cervical scale: wider than long (0); as long as wide (1), cervical absent (2). C45, J70, and Lapparent de Broin *et al.* (2004).

42. Neural series composed of: seven or one bones (0); neurals completely absent (1). C47, D37.
43. Lateral arrangement between neural 1 and 2, and the costal 1 and 2: neural 1 contacts costal 1 and 2, neural 2 only contacts costal 2 (0); neural 1 and costal 1 exclusively in contact between each other, neural 2 only contacts costal 2 (1); neural 1 contacts costal 1 and 2, neural 2 contacts costal 2 and 3 (2); neural 1 only contacts costal 1, neural 2 contacts costal 1 anterolaterally (3). New character.
44. Inguinal buttress: short or absent (0); extends medially to centre of costal 5 (1). G150.

Plastron

45. Mesoplastra: one mesoplastra pair as long as wide, without midline contact, (0); mesoplastra absent (1). Character modified from Cadena & Gaffney (2005).
46. Intergular scale: large, covering the anterior margin of entoplastron, separating the gulars (0); small, restricted between the gulars, lacking contact with entoplastron (1). C53, G170.

